J. Membrane Biol. 163, 55–66 (1998)

The Journal of
Membrane
Biology

The CFTR Chloride Channel: Nucleotide Interactions and Temperature-dependent Gating

C.J. Mathews, J.A. Tabcharani, J.W. Hanrahan
Department of Physiology, McGill University, Montréal, Québec, Canada

Received: 28 August 1997/Revised: 4 February 1998

Abstract. The gating cycle of CFTR (Cystic Fibrosis Transmembrane conductance Regulator) chloride channels requires ATP hydrolysis and can be interrupted by exposure to the nonhydrolyzable nucleotide AMP-PNP. To further characterize nucleotide interactions and channel gating, we have studied the effects of AMP-PNP, protein kinase C (PKC) phosphorylation, and temperature on gating kinetics. The rate of channel locking increased from 1.05×10^{-3} sec^{-1} to 58.7×10^{-3} sec^{-1} when AMP-PNP concentration was raised from 0.5 to 5 mM in the presence of 1 mM MgATP and 180 nM protein kinase A catalytic subunit (PKA). Although rapid locking precluded estimation of P_o or opening rate immediately after the addition of AMP-PNP to wild-type channels, analysis of locking rates in the presence of high AMP-PNP concentrations revealed two components. The appearance of a distinct, slow component at high [AMP-PNP] is evidence for AMP-PNP interactions at a second site, where competition with ATP would reduce P_o and thereby delay locking. All channels exhibited locking when they were strongly phosphorylated by PKA, but not when exposed to PKC alone. AMP-PNP increased P_o at temperatures above 30°C but did not cause locking, evidence that the stabilizing interactions between domains, which have been proposed to maintain CFTR in the open burst state, are relatively weak. The temperature dependence of normal CFTR gating by ATP was strongly asymmetric, with the opening rate being much more temperature sensitive (Q_{10} = 9.6) than the closing rate (Q_{10} = 3.6). These results are consistent with a cyclic model for gating of phosphorylated CFTR.

Key words: Cystic fibrosis — Anion channel — Nucleotide binding — Temperature coefficient — Patch clamp

Correspondence to: J.W. Hanrahan

Introduction

The Cystic Fibrosis Transmembrane conductance Regulator (CFTR) is a membrane protein expressed in epithelial, cardiac and other cells, which functions as a nonrectifying, low-conductance chloride channel (*see* reviews Gadsby, Nagel & Hwang, 1995; Hanrahan et al., 1995). The protein is a member of the ATP-binding cassette (ABC) family (Riordan et al., 1989; Hyde et al., 1990), and consists of two membrane-spanning domains, a regulatory (*R*) domain and two nucleotide binding folds (NBFs). In humans, dysfunction of this channel results in the disease cystic fibrosis (reviewed by Welsh & Smith, 1994).

Normally, in vivo activity of the channel is increased by secretagogues that elevate intracellular cAMP, resulting in protein kinase A (PKA)-mediated phosphorylation at multiple sites (Cheng et al., 1991; Picciotto et al., 1992). Exposure to PKA activates CFTR channels in excised patches (Tabcharani et al., 1991; Berger, Travis & Welsh, 1993), but we recently demonstrated that constitutive protein kinase C (PKC)-catalyzed phosphorylation is also required for acute channel activation (Jia, Mathews & Hanrahan, 1997). Mutation of the 10 ''strong'' dibasic consensus sites present in the CFTR sequence only results in partial loss of PKA-stimulated channel activity (10SA; Chang et al., 1993, Mathews et al., 1998) suggesting that phosphorylation of alternative sites by PKA is sufficient to allow activation. The gating of CFTR requires hydrolyzable nucleotides together with magnesium ions, and there is evidence that both opening and closing transitions are coupled to ATP hydrolysis (Anderson et al., 1991; Baukrowitz, et al., 1994; Gunderson & Kopito, 1994; Dousmanis, Nairn & Gadsby, 1996; Li et al., 1996). The apparent affinity of the 10SA mutant for nucleotides is greatly reduced compared to that of wild-type channels, indicating that phosphorylation of the dibasic PKA sites modulates open probability (P_o) at least in part, through

changes in the ATP-dependence of CFTR (Mathews et al., 1998).

Phosphorylated CFTR channels become ''locked'' in an open burst state when exposed to solutions containing both AMP-PNP and ATP (Gunderson & Kopito, 1994; Hwang et al., 1994; Carson, Travis & Welsh, 1995). This locking behavior has been proposed to involve a stabilizing interaction between the two NBFs (Baukrowitz et al., 1994; Nagel et al., 1994). Interactions between domains may also stabilize open bursts during normal channel gating in the absence of nonhydrolyzable analogue, such that open bursts continue until they are terminated by hydrolysis of the ATP bound at NBF2. ATP hydrolysis at NBF1 probably results in channel opening (Baukrowitz et al., 1994; Carson et al., 1995; Carson & Welsh, 1995). By analogy with other proteins (e.g., F_1-ATPase, Weber & Senior, 1996), interactions between NBFs may influence gating by controlling the rate at which hydrolysis products are released from NBF1 (Baukrowitz et al., 1994; Nagel et al., 1994).

No effect of AMP-PNP on channel opening rate has been reported, although one might expect this analogue to produce a ''locked closed'' state in addition to the ''locked open'' state. Indeed it has been suggested that AMP-PNP does not interact with CFTR at all, and therefore can provide no information regarding nucleotide hydrolysis (Schultz et al., 1995). Also, one would anticipate competition between ATP and AMP-PNP and that they would have opposite effects on channel locking, since when an ATP is bound at NBF2 its hydrolysis would enable channel closure.

To better understand the interactions of nucleotides with the NBFs we have studied CFTR channels in the presence of various mixtures of hydrolyzable and nonhydrolyzable nucleotides. We found that locking rate was dependent on AMP-PNP concentration in a manner consistent with competitive interactions between ATP and AMP-PNP at the locking site. Moreover, the kinetics of locking strongly suggest inhibitory interactions of AMP-PNP at a second site, presumably NBF1. PKC phosphorylation did not support stable locking. The domain interactions proposed to underlie locking are relatively weak, since they were easily overcome by thermal energy. Finally, the activation energies (E_a) for CFTR channel activity were large and asymmetric. This suggests opening and closing transitions have different rate limiting steps, consistent with a cyclic gating scheme. Some of these results have appeared in preliminary form (Mathews et al., 1995; Mathews et al., 1996).

Materials and Methods

Cell Culture

Chinese hamster ovary cells stably expressing CFTR were plated at a density of ~500,000/cm^2 on glass coverslips and used 3–5 days later. Cultures were maintained in DMEM supplemented with 8% FBS, penicillin (100 U.mL^{-1}) and streptomycin (100 μg.mL^{-1}) and methotrexate (100 μM) in a humidified 5% CO_2 atmosphere at 37°C. Media constituents were from GIBCO (Burlington, ONT).

Solutions and Chemicals

Cells were placed in a recording chamber containing (mM): 150 NaCl, 2 $MgCl_2$, 10 TES, pH 7.4. In all experiments the nonhydrolyzable nucleotide, adenylyl-imidodiphosphate (AMP-PNP; Tetralithium salt) was added to the bath from a 100 mM stock solution in buffer (150 NaCl and 10 TES, with final pH adjusted to 7.4 using 1 N NaOH), yielding final concentrations of 0.25–5 mM as indicated. MgATP was present from the start of experiments at concentrations of 0.25–5 mM. MgATP was added from a stock solution in 150 NaCl and 10 TES, with final pH adjusted to 7.4 with 1 N NaOH. Chemicals were from Sigma Chemical (St. Louis, MO). Catalytic subunit of PKA was usually present in the bath at a concentration of 180 nM (provided by Dr. M.P. Walsh, University of Calgary, Alberta, Canada; *see* Tabcharani et al., 1991 for details). For experiments involving low PKA activity, the enzyme was used at a final concentration of 17.8 nM (from Promega, Madison, WI). Rat brain PKC, which is comprised of Ca^{2+}- and phospholipid-dependent PKC isoforms, was also prepared in the laboratory of Dr. M.P. Walsh (*see* Tabcharani et al., 1991). When PKC (3.7 nM) was used, the lipid cofactor, 1,2-dioctanoyl-*rac*-glycerol (DiC:8) was also added to the bath at 5 μM final concentration. DiC:8 was dissolved in chloroform at 10 mM and stored at −20°C under nitrogen before use.

Electrophysiology

Experiments were performed using the inside-out configuration of the patch-clamp technique (Hamill et al., 1981). Pipettes were prepared using a conventional puller (PP-83, Narishige Instrument, Tokyo) and had resistances of 4–6 MΩ when filled with 150 mM NaCl solution. The bath solution was grounded through an agar bridge having the same ionic composition as the pipette solution. Single-channel currents were amplified (Axopatch 1C, Axon Instruments, Foster City, CA), recorded on video cassette tape by a pulse-coded modulation-type recording adapter (DR384, Neurodata Instrument, NY) and low-pass filtered during play back using an 8-pole Bessel-type filter (900 LPF, Frequency Devices, Haverhill, MA). The final recording bandwidth was 230 Hz (−3 dB), and records were sampled at 1 kHz and analyzed using a microcomputer as described previously (Tabcharani et al., 1991) or using the DRSCAN program running on a PC (Hanrahan et al., 1998). All patches were studied with the pipette potential clamped at +30 mV (i.e., membrane potential V_m = −30 mV). The single-channel open probability (P_o) was calculated as:

$$P_o = (<I> / i) / N \quad (1)$$

where $<I>$ is the mean current through the patch mediated by CFTR channels and i is the unitary current flowing through a single open channel. N is the number of channels counted in the patch after addition of AMP-PNP (*see* below). The number of opening transitions during each segment (>120 sec) was counted and used to estimate the mean burst (τ_{open}) and interburst (τ_{closed}) durations according to:

$$\tau_{open} = (N \cdot P_o)\ (T) / (\#\ \text{of openings}) \quad (2)$$

$$\tau_{closed} = (N - N \cdot P_o)\ (T) / (\#\ \text{of closures}) \quad (3)$$

where N is the number of channels, P_o is the single-channel open probability, and T is the duration of the segment (*see* Gray, Greenwell

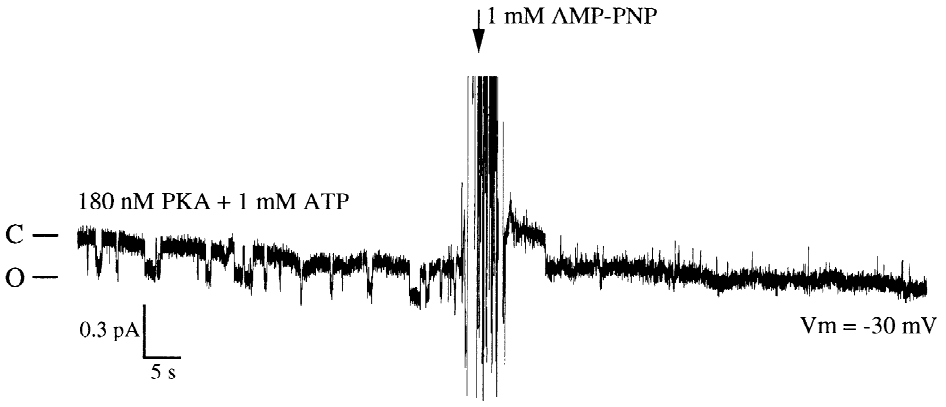

Fig. 1. Typical ''locking'' behaviour in a patch containing a single CFTR channel. Openings are downwards in this and all subsequent figures (V_m = −30 mV). Note that the channel becomes rapidly and stably locked open following addition of 1 mM AMP-PNP to the recording chamber, which already contains 180 nM PKA and 1 mM MgATP.

& Argent, 1988). Although this approach for calculating burst durations in multichannel patches assumes only two kinetic states (open and closed), there is good agreement between the slow (i.e., burst) kinetics measured by cycle times, and those determined for single-channel patches using the threshold crossing method when flickery closures within bursts are excluded from the analysis (*see* Mathews et al., 1998). The number of functional channels in the patch (*N*), which is required when calculating open probability and mean interburst duration (Eqs. 1 and 3), was determined at the end of each experiment by locking the channels open with AMP-PNP. To calculate the rate of locking, the latencies (in seconds) between the time of AMP-PNP addition and the time at which each channel in a patch became locked open was determined (*see* Mathews et al., 1998). Unless stated otherwise studies were carried out at room temperature (~23°C).

Temperature Dependence

The recording chamber used to study the effects of temperature had a bottom coated with transparent indium tin oxide (HI-25x; Cell MicroControls, Virginia Beach, VA). This heater was connected to a temperature controller (TC-1; Cell MicroControls). Bath temperature was monitored using a miniature thermistor probe (TH-2Km, 0.45 mm diameter; Cell MicroControls) lying flat against the bath bottom and connected to a Tele-Thermometer (YSI, Yellow Springs, OH). Baseline patch current was stable within 90 sec after a step increase in the temperature set point. The temperature dependence of the open burst and interburst durations was described by the temperature coefficient, Q_{10}, which was calculated according to the equation:

$$Q_{10} = [X_1/X_2] \times [10/(T_2 - T_1)] \quad (4)$$

where X_1 is the value of the parameter at T_1 (e.g., opening rate at the lower temperature, 23°C), and X_2 is the value of the parameter at T_2 (e.g., opening rate at the higher temperature, 37°C). Arrhenius plots were graphed as: ln(*X*) *vs.* $1/T\ (K^{-1})$ where *X* is the channel parameter and *T* is the temperature. Energies of activation (E_a; $kJ.mol^{-1}$) for the channel closing and opening rates and conductance were determined from the slopes of Arrhenius plots as follows:

$$E_a = -Slope \cdot R \quad (5)$$

where *R* is the gas constant (8.314 $J.mol^{-1}.K^{-1}$).

Statistics

Data are shown as mean ± standard error (SEM) throughout, and were tested for statistical significance ($P < 0.05$) using the paired or unpaired Student's *t*-test as appropriate (InStat; GraphPad, Biosoft, Cambridge, UK). Data were plotted and, where appropriate, fitted using Origin (version 4.1; Microcal Software, Northampton, MA).

Results

CFTR chloride channels became stably ''locked'' in the open-burst state at 23°C when the nonhydrolyzable nucleotide AMP-PNP was added to patches in the presence of PKA (180 nM) and MgATP (1 mM; Fig. 1). The number of channels locked open was always equal to, or greater than, the maximum number simultaneously open in the preceding control traces (in the presence of PKA and MgATP alone). This locking of CFTR channels requires PKA-mediated phosphorylation, although phosphorylation of a mutant lacking the 10 ''strong'' dibasic PKA consensus sites (10SA) is sufficient for stable locking when PKA activity is high (180 nM; Mathews et al., 1998). When we tested the effect of AMP-PNP (1 mM) on channels stimulated by excision into a bath containing 3.7 nM PKC, they did not become progressively locked (Fig. 2*A*), although P_o increased significantly (from 0.034 ± 0.0125 to 0.289 ± 0.0592; $n = 4$; $P = 0.012$) due to increases in burst duration (from 0.357 ± 0.029 sec to 1.524 ± 0.208 sec; $n = 4$; $P = 0.008$). Interburst durations were highly variable but not altered significantly by AMP-PNP (18.47 ± 7.059 s before and 4.48 ± 1.341 s after addition; $n = 4$; $P > 0.2$). Also, as shown in Fig. 2*B*, no locking was observed when a low concentration of PKA was used (17.8 nM). These results confirm that if domain interactions underlie stable locking, the interactions require phosphorylation. Moreover, PKC or weak PKA phosphorylation under these condi-

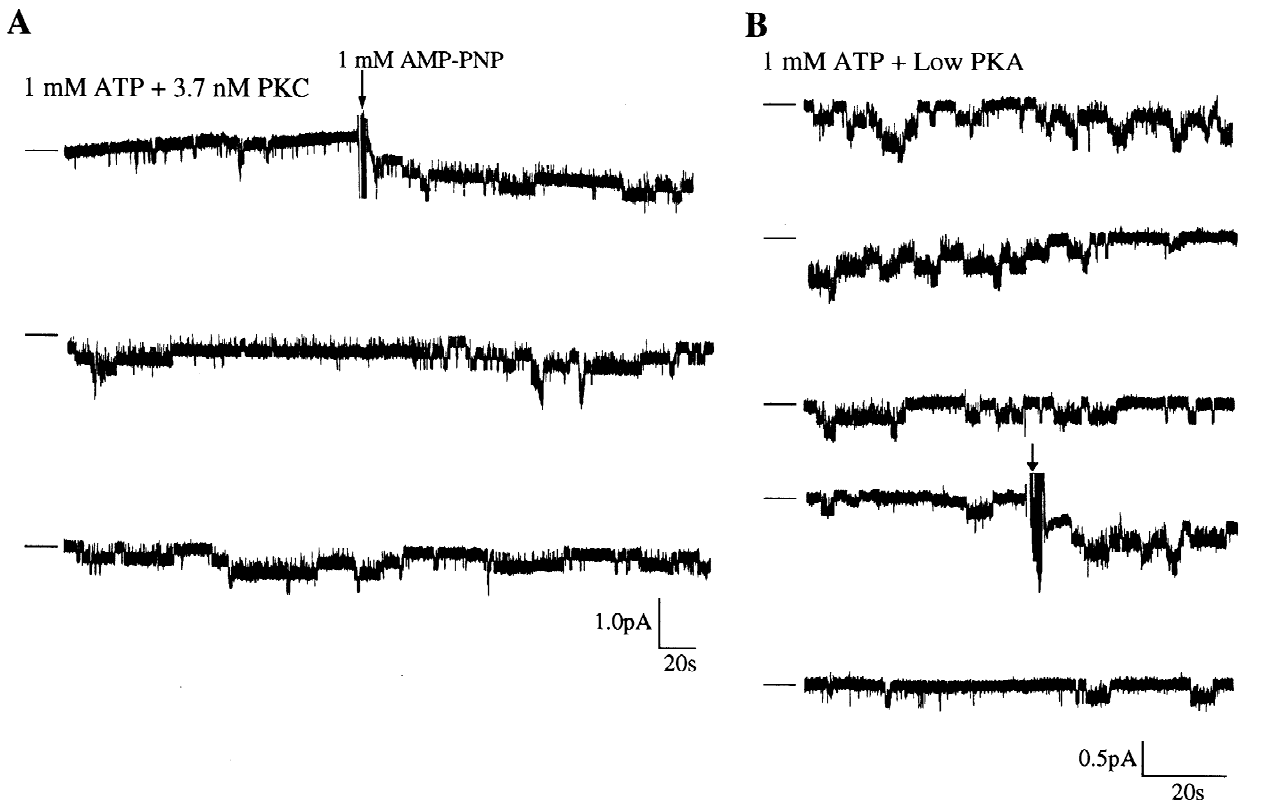

Fig. 2. (*A*) Channels stimulated by PKC are not locked open by AMP-PNP. An 18-min record from a patch stimulated with PKC (3.7 nM) in the presence of MgATP (1 mM) and DiC:8 (5 μM). Following addition of AMP-PNP (1 mM), P_o and τ_{open} both increased significantly (*see* text) but channels did not become stably locked in the open burst state. Traces shown are typical of $n = 4$ experiments. (*B*) Channels stimulated by a low concentration of PKA are not locked open by AMP-PNP. Effect of adding 1 mM AMP-PNP (arrow) to a patch containing activity of CFTR channels in response to weak PKA-mediated stimulation (17.8 nM). Locking was not observed despite the continuous presence of PKA, MgATP and AMP-PNP. Solid line to the left of each trace indicates the current level when all channels are closed.

tions fail to mimic the effect of strong phosphorylation by PKA.

To further characterize nucleotide interactions we varied the concentrations of ATP and AMP-PNP in the bath solution. In each experiment, MgATP and PKA were present from the start, and AMP-PNP was added after recording several minutes of control activity. The latencies between addition of AMP-PNP and the locking of each channel were ranked in descending order, plotted on an exponential scale, and fitted by linear regression with single exponentials as described previously for AMP-PNP (Mathews et al., 1998) and similar to the cumulative distribution for orthovanadate locking described by Baukrowitz et al. (1994). As discussed previously (Mathews et al., 1998) the rates calculated by this method yield a locking rate, not a true *on-rate* for AMP-PNP, since channel locking apparently occurs only from the open state. However, our measurement of the *locking* rate (based on the time between the addition of AMP-PNP and the time at which single channels become locked open) is still a valid measurement for both single-channel and multi-channel patches. To estimate on-rates for AMP-PNP, one would multiply the latencies for individual channels by their corresponding P_o values (measured during the control periods immediately after addition of AMP-PNP, when this is technically feasible). When the concentration of AMP-PNP was increased in the range 0.5–5 mM while maintaining [ATP] at 1 mM, the rate at which channels became locked in open bursts was increased (Fig. 3).

Interestingly, a ''break'' appeared in the $P_{unlocked}$-*vs.*-time plot when the final AMP-PNP concentration was greater than 2 mM. As shown in Fig. 4*A* these plots were fit well by a double exponential. Figure 4*B* illustrates the two exponential components seen with 4 mM AMP-PNP. The slow component was observed whenever the AMP-PNP concentration was elevated above 1 mM in the presence of 1 mM ATP. The simplest explanation for the slow locking component is that AMP-PNP interacts at a site which reduces the channel opening rate. Locking was too rapid to test this using wild-type channels, but evidence for such an inhibitory effect of AMP-PNP was obtained using the low-phosphorylation mutant 10SA, which locks slowly enough to allow measurement

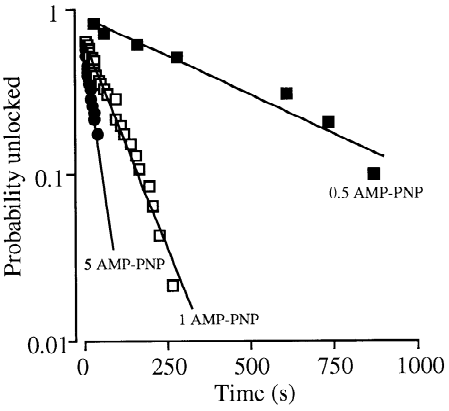

Fig. 3. Effect of increasing AMP-PNP concentration on the locking rate. MgATP concentration was 1 mM throughout. Plots of the probability of a channel being unlocked ($P_{unlocked}$; *see* text) *vs.* time following the addition of AMP-PNP. Data were fitted by exponential functions to determine locking rates. Only early time points are plotted for 5 mM AMP-PNP (*see* Fig. 4). The data shown in these plots were obtained as follows: 0.5 mM AMP-PNP (8 channels, 3 patches); 1 mM (47 channels, 6 patches) and 5 mM AMP-PNP (46 channels, 7 patches).

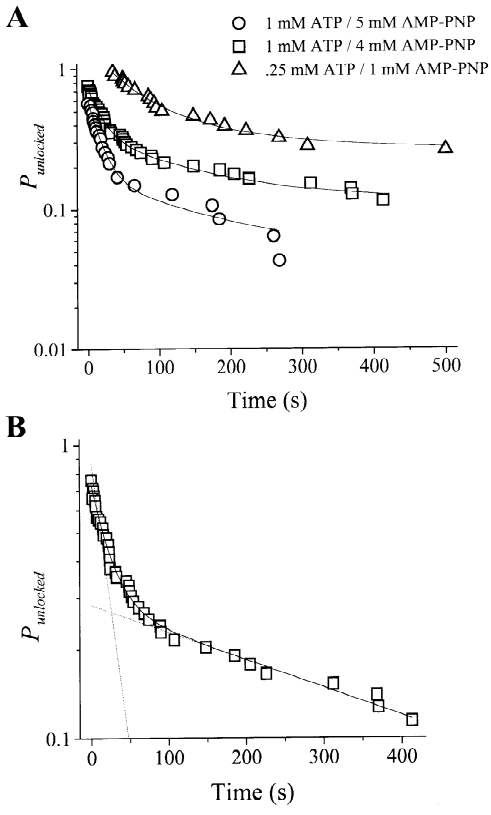

Fig. 4. A slow component appears in the probability density function when the concentration of AMP-PNP is greater than the ATP concentration, (*A*). Plots of the $P_{unlocked}$-*vs.*-time data with 4 or 5 mM AMP-PNP show a break in the linear relationship caused by the development of a slow component. Also shown are data obtained when channels were locked open by 1 mM AMP-PNP in the presence of 0.25 mM ATP. Data in these plots were obtained as follows: 4 mM AMP-PNP and 1 mM ATP (79 channels, 6 patches), 5 mM AMP-PNP and 1 mM ATP (46 channels, 7 patches) and 1 mM AMP-PNP and 0.25 mM ATP (25 channels from 4 patches). Locking rates were obtained by fitting data with second-order exponential functions. The fit amplitudes for the fast and slow locking components were as follows (in mM): 4 AMP-PNP + 1 ATP, 0.401 (fast), 0.222 (slow); 5 AMP-PNP + 1 ATP, 0.440 (fast), 0.126 (slow); and 1 AMP-PNP + 0.25 ATP, 0.4027 (fast), 0.2858 (slow). (*B*) Plot of $P_{unlocked}$-*vs.*-time data illustrating the two components. Data obtained in the presence of 4 mM AMP-PNP are shown together with exponential fits (dotted lines). The fast locking rate was 45.3×10^{-3} sec^{-1}, while the slow rate was 2.2×10^{-3} sec^{-1}.

of P_o after adding AMP-PNP. As shown in Fig. 5, there was a decrease in NP_o immediately after adding AMP-PNP to 10SA channels in the presence of 1 mM MgATP, 180 nM PKA and 2 mM $MgCl_2$, consistent with competitive inhibition of ATP-dependent opening.

When the concentration of AMP-PNP and ATP were altered such that their ratio was maintained at unity, then varying [AMP-PNP] had a very different effect from that described above. Channels exposed to high concentrations of both nucleotides had relatively slow locking rates (Fig. 6*A*). In fact, there was an inverse relationship between the rate of locking and [AMP-PNP] under these conditions, with the locking rate decreasing from 13.1×10^{-3} sec^{-1} at 0.5 mM AMP-PNP to 1.37×10^{-3} sec^{-1} at 5 mM AMP-PNP (Fig. 6*A*). When compared with data in Fig. 4, these results strongly suggest that ATP delays locking through competition with AMP-PNP at the locking site, since the only difference between these experiments and the previous ones was the parallel elevation of [ATP]. Figure 6*B* illustrates the complex relationship between nucleotide concentration and stabilization of the open state. Locking was rapid when the concentrations of both nucleotides were 0.5 mM. Increasing ATP concentration to 1 mM while maintaining AMP-PNP at 0.5 mM greatly reduced the rate of locking from 13.1 to 1.05×10^{-3} sec^{-1} (12-fold reduction). Elevating the AMP-PNP concentration to 1 mM (so that a 1:1 ratio was restored) caused the locking rate to increase by 11-fold to 11.5×10^{-3} sec^{-1}, similar to that observed with low concentrations of both nucleotides. Thus, even over the range 0.5 to 1 mM, the rate of locking is greatly reduced by elevating ATP and enhanced by raising AMP-PNP. The data shown in Fig. 6*A* also suggest that the affinity of the locking site for ATP may be somewhat higher than for AMP-PNP, since increasing the concentrations of both nucleotides slowed the rate of channel locking. This is also apparent in Fig. 6*B*, which shows that locking is faster when both nucleotides are 0.5 mM rather than 1 mM.

The effects of AMP-PNP on CFTR activity have been controversial. Some variability between studies could reflect differences in temperature if the stabilizing interactions which are thought to underlie locking are weak and thus easily overcome by thermal energy. To

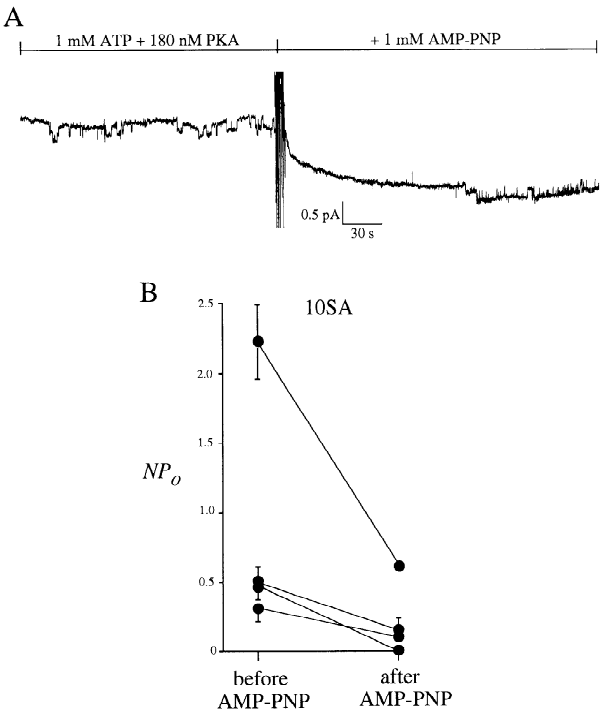

Fig. 5. Partial inhibition of 10SA-CFTR following AMP-PNP addition suggesting an inhibitory effect of AMP-PNP. (*A*) Continuous current trace showing activity of two 10SA channels before and after the addition of 1 mM AMP-PNP. MgATP (1 mM) and PKA (180 nM) were present throughout. (*B*) Plot showing decrease in channel activity (NP_o) following addition of AMP-PNP (1 mM). For each patch ($n = 4$) mean NP_o was measured for >120 sec before addition of AMP-PNP, and then in the period between the addition of AMP-PNP and the time that channels locked open.

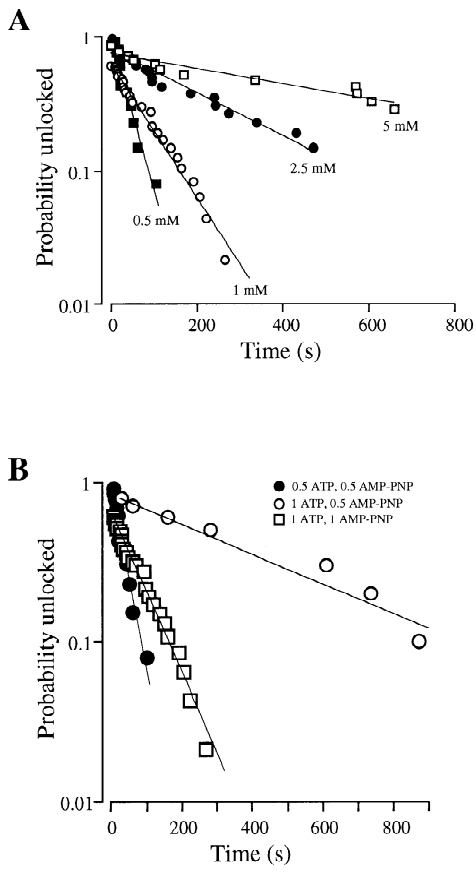

Fig. 6. Dependence of locking rate upon nucleotide concentrations suggests competition for the locking site. (*A*) Inverse relationship between concentration and locking rate when [AMP-PNP]:[ATP] = 1. Plots of P_{unlocked}-*vs.*-time at various concentrations of both AMP-PNP and ATP. Data for 1 mM ATP and 1 mM AMP-PNP are as shown in Fig. 3. For the other mixtures, the concentrations of each nucleotide and number of patches are as follows (in mM): 0.5 each (13 channels, 4 patches); 2.5 each (26 channels, 5 patches) and 5 (21 channels, 6 patches). (*B*) Plots of P_{unlocked}-*vs.*-time in the presence of (in mM): 0.5 ATP and 0.5 AMP-PNP (13 channels, 4 patches), 1 ATP and 0.5 AMP-PNP (8 channels, 3 patches) or 1 ATP and 1 AMP-PNP (47 channels, 6 patches).

test this, we examined the effects of changing the bath temperature on the behavior of channels that had been locked open using AMP-PNP. Temperature was raised from 23°C to 37°C (Fig. 7). Channels that had been locked open by 1 mM AMP-PNP at 23°C began unlocking when the temperature reached 30°C. At this temperature prolonged bursts were still observed in the continued presence of ATP and AMP-PNP, although they were no longer apparent when the temperature reached 37°C. P_o was elevated compared with channels at the same temperature (37°C) without AMP-PNP (P_o with AMP-PNP = 0.833 ± 0.046; $n = 3$; P_o in absence of AMP-PNP = 0.656 ± 0.024; $n = 4$; $P = 0.014$). Addition of a similar concentration of ATP (1 mM) instead of AMP-PNP would have had little effect on P_o (*see* below). Thus locking at room temperature is overcome by raising the temperature moderately, however some stabilization by AMP-PNP must still occur since P_o is increased.

Finally, we investigated the temperature-dependence of CFTR gating when channels were bathed with 1 mM MgATP and 180 nM PKA. Raising the temperature from 23°C to 30°C increased the P_o and decreased both the burst and interburst durations significantly (Table). Elevating the temperature to 37°C further decreased the open and closed times when compared to values obtained at 23°C or 30°C, although P_o was not significantly different from that at 30°C (*see* Table and Fig. 8). Interestingly, the effects on burst and interburst durations were quantitatively very different. The Q_{10} for mean open burst duration was 3.6 while that for the mean interburst duration was 9.6. Thus the opening rate (reciprocal of mean interburst duration) was more temperature-sensitive than the closing rate. Figure 9 compares Arrhenius plots for the opening and closing rates and single-channel conductance. The plots appeared linear and were fit by first order regression. By contrast, P_o,

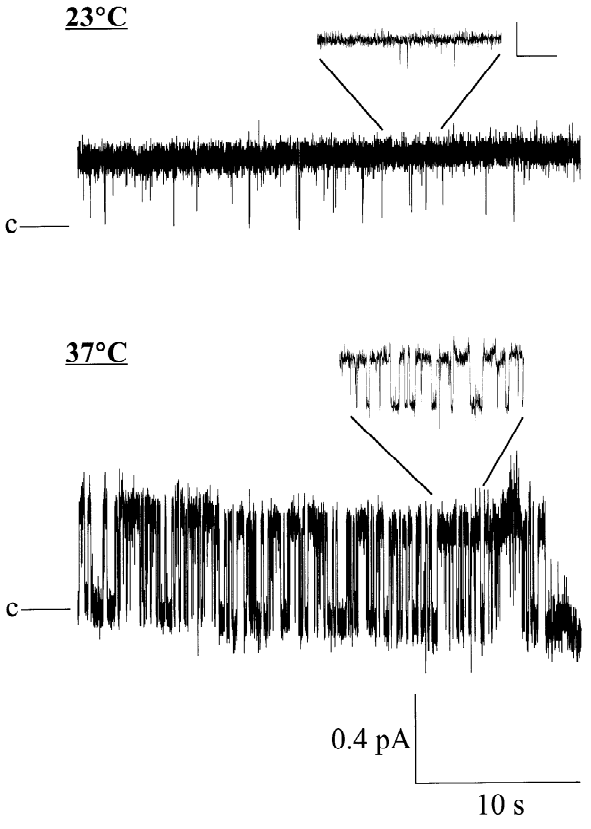

Fig. 7. Raising bath temperature destabilizes locking. In the patch shown, a single channel became locked open at room temperature (23°C) after the addition of 1 mM AMP-PNP. PKA (180 nM) and MgATP (1 mM) were present throughout. Increasing bath temperature caused the channels to begin unlocking, and at 37°C no prolonged openings were apparent, as illustrated by the expanded trace above the channel record (scale bar for expanded traces represents 0.3 pA and 0.75 sec).

which is a function of both opening and closing rates, was more complex, showing a greater temperature sensitivity between 23 and 30°C than over the range 30–37°C. The activation energies (E_as; *see* Table) estimated for entering and leaving the open burst state were large and very different from each other; channel opening was significantly more temperature sensitive than channel closing.

Discussion

To better understand the interactions of nucleotides with the NBFs, we have examined the locking behavior of CFTR chloride channels exposed to mixtures of hydrolyzable and nonhydrolyzable nucleotides. The rate of locking was proportional to AMP-PNP concentration. Comparison of the results obtained when [ATP] was fixed at 1 mM or was allowed to vary with [AMP-PNP] indicated competition between ATP and AMP-PNP at the locking site (proposed to be NBF2). Moreover, high AMP-PNP concentrations introduced a slow component into the locking time histograms. Since wild-type channels can only be locked by AMP-PNP when they are open (Hwang et al., 1994; Mathews et al., 1998), slow locking probably reflects a reduction in P_o caused by competition between AMP-PNP and ATP at the other NBF (probably NBF1). This effect could be demonstrated directly using the 10SA mutant but not wild-type CFTR. Neither PKC nor low PKA were able to support stable locking. Finally, we found that the E_a values for channel closing and opening are large and display a marked asymmetry.

Locking Open Involves Tight Binding or Perhaps Occlusion of AMP-PNP

Highly phosphorylated CFTR channels were consistently locked in open bursts by AMP-PNP, as shown previously using guinea pig ventricular myocytes (Hwang et al., 1994) and human CFTR incorporated into planar lipid bilayers (Gunderson & Kopito, 1994; Carson et al., 1995; but *see* Schultz et al., 1995). The stimulatory effect of AMP-PNP + ATP on macroscopic Cl^- current across permeabilized sweat duct may also be due to such a mechanism (Reddy & Quinton, 1994). It has been proposed that interactions between the NBFs stabilize bursts during normal gating (i.e., in the absence of AMP-PNP), and that each burst continues until it is terminated by hydrolysis of the ATP which is bound at NBF2. This proposed mechanism resembles that of G-proteins, which remain active while GTP is bound and become inactivated following GTP hydrolysis. The NBFs of CFTR share G-protein-like motifs (Manavalan et al., 1995). Mutations in one of these motifs alters CFTR channel function as predicted from studies of G-proteins (Carson & Welsh, 1995).

CFTR channels remained locked for 20–34 min after washing AMP-PNP from the bath, indicating that the off-rate for AMP-PNP is extremely slow at room temperature. This result agrees with a previous study in which a CFTR channel remained locked open for 18 min following removal of both ATP and AMP-PNP (Hwang et al., 1994). Further studies should determine whether the slow off-rate for AMP-PNP is due to high affinity binding or to a conformational change that traps AMP-PNP (occlusion).

Requirements for Locking Open

In the present work we found that PKC-mediated phosphorylation does not support stable locking of the CFTR channel nor does exposure to low PKA concentration. Performing definitive experiments with low PKA activity was difficult; in most patches either strong channel activation was observed or there was none. Moreover,

Table. Effect of temperature upon single channel properties

Temperature (°C)	Open probability (P_o)	τ_{open} (S)	τ_{closed} (S)	Conductance (pS)
23	0.41 ± 0.026 (5)	1.21 ± 0.099 (5)	1.76 ± 0.159 (5)	8.29 ± 0.14 (7)
30	0.61 ± 0.034$^{\#}$ (5)	0.62 ± 0.066$^{\#}$ (5)	0.41 ± 0.066* (5)	10.62 ± 0.23* (5)
37	0.66 ± 0.024* (4)	0.24 ± 0.019** *(4)	0.13 ± 0.024$^{\#\#}$* (4)	12.56 ± 0.76†† * (4)
		$1/\tau_{open}$ (sec^{-1})	$1/\tau_{closed}$ (sec^{-1})	Conductance (pS)
Q_{10}		3.6	9.6	1.1
E_a ($kJ.mol^{-1}$)		87.3	145.5	22.5

* and $^{\#}$: Significantly different from corresponding value at 23°C. (*$P < 0.0002$; $^{\#}P < 0.002$).
, $^{\#\#}$ and ††: Significantly different from corresponding value at 30°C. ($P < 0.002$; $^{\#\#}P < 0.01$ and ††$P < 0.05$).
Values are means ± SEM and numbers in parentheses indicate the number of patches analyzed under each experimental condition. At each temperature, the single-channel point conductance was calculated from the current amplitude measured at V_m −30 mV. Temperature coefficients (Q_{10}) and energies of activation (E_a) were calculated as described in Materials and Methods.

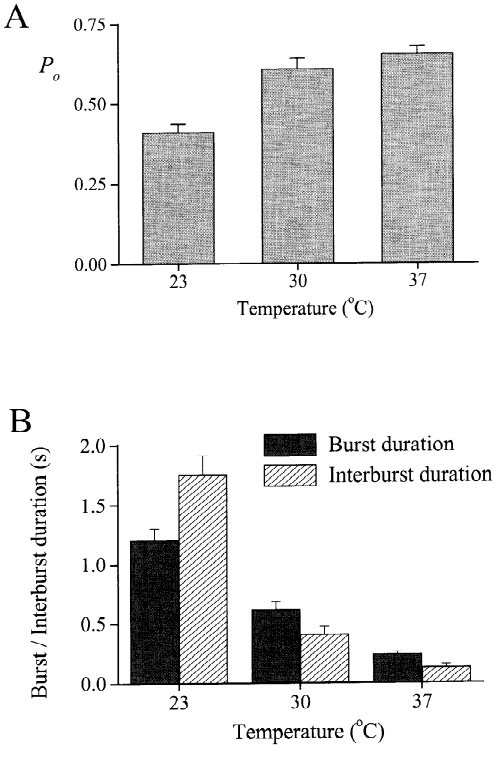

Fig. 8. Effects of temperature upon CFTR channel kinetics in the absence of AMP-PNP. (*A*) Plot of open probability *vs.* temperature of the bath solution. (*B*) Plot of open burst and interburst durations against temperature. Both burst and interburst durations declined when the temperature was increased, however the reduction in interburst duration was larger, as illustrated by the temperature coefficients (Q_{10}) shown in Table 1. The mean recording length at each temperature was 233 ± 33 s at 23°C ($n = 5$), 248 ± 47 s at 30°C ($n = 5$) and 132 ± 26 s ($n = 4$) at 37°C. *See* Table 1.

considerable time was required for channels to reach a steady-state level of activity with low PKA, as during the first 2–3 min of the trace shown in Fig. 2*B*. We can only speculate that when initially exposed to low PKA, sites may become transiently phosphorylated and then slowly dephosphorylated as phosphatases (which are associated with the patch and may have slower enzyme kinetics) cause partial rundown. The fact that, in the experiment shown, addition of AMP-PNP caused four channels to be open simultaneously (albeit only for a few seconds) suggests that the CFTR channels were in a lockable state, but that locking was not achieved because critical sites were not phosphorylated under these conditions.

The effects of low [PKA] have interesting implications for the phosphorylation dependence of locking. We showed recently that the 10SA mutant could still be locked when exposed to high [PKA]. Unidentified cryptic sites can thus support locking if the PKA activity is sufficient to maintain at least one such low affinity site phosphorylated despite the presence of phosphatases. By contrast, the low kinase activity used in this experiment (Fig. 2*B*) was apparently not sufficient to maintain the sites phosphorylated. We note that synthetic peptides containing different PKA consensus sequences from CFTR can vary 12-fold in their effectiveness as kinase substrates, as estimated from the ratio of k_{cat}/K_M (Picciotto et al., 1992). The exact mechanism of locking remains speculative; PKA-dependent phosphorylation may enhance stabilizing interactions between NBFs that prevent AMP-PNP dissociation. If domain-domain interactions underlie locking, they may be relatively weak since locking was overcome by elevating the temperature by only 7°C.

Alternatively, the off-rate for AMP-PNP may depend more directly on phosphorylation of critical PKA sites. These could be monobasic or cryptic sites, since the 10SA mutant can be locked in the presence of high PKA activity (Mathews et al., 1998).

Evidence that AMP-PNP Interacts with Both NBFs

Hydrolysis of ATP by NBF1 and NBF2 has previously been suggested to enable opening and closing transitions, respectively, therefore we expected a non-hydrolyzable

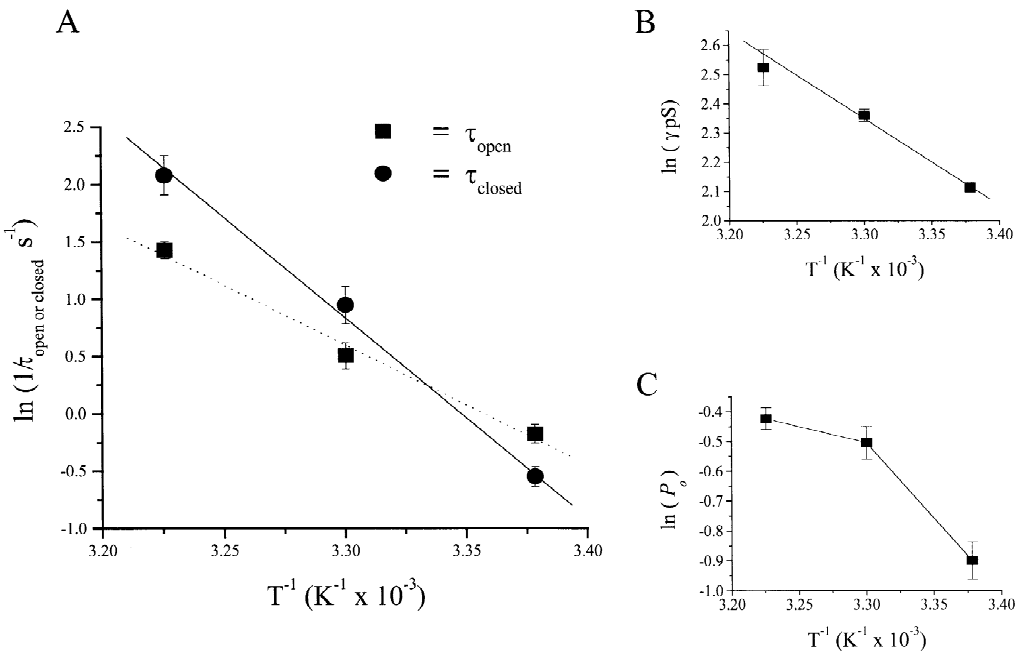

Fig. 9. Arrhenius plots of single channel kinetic parameters. (*A*) Semi-log plots of closing and opening rates ($1/\tau_{open}$ and $1/\tau_{closed}$, respectively) *vs.* the reciprocal of temperature (K^{-1}). Data were fit by linear regression ($1/\tau_{open}$, $r^2 = 0.998$; $1/\tau_{closed}$, $r^2 = 0.997$). Energies of activation (E_a) were obtained from the slopes. (*B*) Semi-logarithmic plot of single-channel conductance (γ) *vs.* the reciprocal of temperature. Data were fit by linear regression ($r^2 = 0.996$). (*C*) Semi-log plot of single-channel open probability (P_o) *vs.* the reciprocal of temperature. Data points are connected by straight lines. (Values for all parameters are contained in Table 1).

nucleotide to have opposite effects on P_o depending on whether it happened to bind at NBF1 or NBF2. A direct test would be to measure P_o and interburst durations immediately after adding AMP-PNP (before the channel became locked open), however rapid locking of wild-type channels precluded those measurements. Nevertheless, elevating bath AMP-PNP concentration above that for ATP led to a slow component in the distribution of locking times. Since the locking rate is proportional to P_o (Mathews et al., 1998), this slow component at high AMP-PNP concentrations suggests an inhibitory effect of AMP-PNP on channel opening, which would decrease P_o and thus locking rate. Moreover, direct inhibition of CFTR activity by AMP-PNP prior to locking was observed in studies of 10SA channels, which lock slowly enough to allow measurement of P_o (Fig. 5). If AMP-PNP delays locking by interacting with CFTR, the most obvious candidate site for this effect would be NBF1. Taken together, these results provide the first evidence that nonhydrolyzable nucleotides can inhibit CFTR channel opening.

We should consider the possibility that two locking components appear after addition of AMP-PNP because it reduces free Mg^{2+} and MgATP concentrations, and thus P_o. For example, channels that were already open when AMP-PNP was added may represent one population of channels, and those that opened (at the new, lower P_o in the presence of AMP-PNP) and locked following the addition of AMP-PNP a second population. One might expect the latencies of these two populations to reflect their different P_o values, since locking should only occur from the open state (Hwang et al., 1994; Mathews et al., 1998). However, this explanation for the two components seems unlikely for the following reasons. First, since P_o is ~0.25, we would expect no more than 25% of the channels to be in the fast-locking population. By contrast, we found that most channels locked rapidly, and raising [AMP-PNP] accelerated both fast and slow locking rates. When 4 mM AMP-PNP was added in the presence of 1 mM ATP the fast locking component predominated over the slow locking rate (64.4% *vs.* 35.6%). When 5 mM AMP-PNP was added the fast rate component was even larger (77.7%); in both cases the predominant locking component was fast. Second, one would expect a small drop in P_o to cause only a modest decrease in the locking rate, but we found the slow component to be >8-fold slower. The slow component was not caused by high AMP-PNP concentration *per se*, since it also appeared when only 1 mM AMP-PNP was added in the presence of 0.25 mM ATP (Fig. 4*A*). Since 2.25 mM Mg^{2+} was present in the experiments with low AMP-PNP, those results also provide further evidence against a decrease in Mg^{2+} being responsible for the appearance of two components. Thus increasing the AMP-PNP:ATP concentration ratio causes a subpopulation of channels to be locked open at a slower rate.

In addition to interacting with the site that mediates channel opening (NBF1), hydrolyzable and nonhydrolyzable nucleotides would be expected to compete at the other site, where ATP hydrolysis terminates open bursts (NBF2). Our results indicate that this is indeed the case, since raising [ATP] slowed the rate of locking in a manner consistent with competition. The EC_{50} of NBF2 for ATP may be lower than for AMP-PNP since locking was rapid at low concentrations of ATP and AMP-PNP, and increasing the concentration of both nucleotides whilst maintaining their ratio at unity dramatically slowed the locking rate (Fig. 6*A*). In this context EC_{50} refers to the nucleotide concentration at which ''NBF2 function'' is 50% of that observed with saturating levels of the nucleotide. This would not be equivalent to ATP affinity (or on-rate) because it depends on the rates of association and dissociation and also k_{cat}. Further studies are required to determine the affinity of each nucleotide for the locking site.

Effects of Thermal Energy on Conductance and Gating

CFTR channel conductance appeared slightly less temperature sensitive in this study (Q_{10} = 1.1) compared to previous reports (~1.3; Tabcharani et al., 1990; Schultz et al., 1995) but was within measurement error of the value expected for free solution. Studies of other ion channels have suggested similar Q_{10}s for single-channel conductance although values ranging between 1.0 and 2.5 have been reported (*see* Hille, 1992). Examples include 1.21 for connexin40 gap-junctional channels (Bukauskas et al., 1995), 1.25 for cardiac K^+_{ATP} channels (Haverkampf, Benz & Kohlhardt, 1995) and 1.28 for neuroblastoma Na^+ channels (Nagy, Kiss & Hof, 1983).

Raising the temperature should affect kinase and phosphatase activities, however small changes in phosphorylation would probably not affect the time constants substantially since reducing total phosphorylation by >90% increases mean interburst duration by only twofold and has no effect on burst duration (Mathews et al., 1998). Indeed, parallel increases in PKA and phosphatase activities at 30 and 37°C might well cancel, leaving steady-state phosphorylation of CFTR relatively unchanged. The values we obtained at 37°C for mean burst (0.24 sec) and interburst duration (0.13 sec) agree with those of Carson et al. (1995) at 34–36°C (burst duration = 0.21 sec, interburst duration = 0.19 sec). CFTR in their experiments was transiently expressed in HeLa cells and studied in excised patches in the presence of 1 mM ATP and 75 nM PKA. Thus under these conditions, the level of CFTR activity appears to be relatively independent of the cell system used.

Temperature dependence can provide information relevant to the mechanism of channel gating. The slow gate of the multimeric C1C-0 chloride channel is exquisitely temperature sensitive (Q_{10} ~40), and this sensitivity has been interpreted as evidence for a complex rearrangement among subunits (Pusch, Ludewig & Jentsch, 1997). Since bursts of the CFTR channel are initiated and terminated by nucleotide hydrolysis, we expected channel opening and closing rates to have large activation energies (E_a) comparable with those of other ATPases (*see* below). The present results show that CFTR channel gating is indeed highly temperature sensitive, yielding E_a values for channel opening and closing transitions of 145.5 and 87.3 $kJ.mol^{-1}$, respectively. The marked asymmetry in Q_{10} values is consistent with, but not proof of, a cyclic gating scheme, since it implies different rate limiting steps for entering and leaving the open burst state rather than a single, reversible transition.

Although similar to known ATPases, the temperature sensitivity of CFTR gating is high when compared with ion channels other than C1C-0. Mammalian cardiac K^+_{ATP} channels have two closing rate constants with Q_{10}s of 1.4–2.9 (Haverkampf et al., 1995). Voltage-gated Ca^{2+} channels have Q_{10}s of 5.9 and 2.0 for opening and closing rates, respectively (Acerbo & Nobile, 1994), whereas those for Na^+ current activation and deactivation rates were 2.2 and 2.9, respectively (Schwarz & Eikhof, 1987). Activation and inactivation rates for $GABA_B$ currents have Q_{10}s between 1.8 and 2.3 (Otis, DeKoninck & Mody, 1993). The high Q_{10}s obtained for CFTR are compatible with ATP hydrolysis reactions as the rate limiting steps for entering and leaving the open burst state. The activation energies for CFTR gating (87 and 146 $kJ.mol^{-1}$) are within the range of values reported for other ATP- and GTP-ases studied at similar temperatures including (in $kJ.mol^{-1}$): the Na^+/K^+-ATPase pump current (92; Friedrich, Bamberg & Nagel, 1996), cardiac actomyosin ATPase (105–125; Siemankowski, Wiseman & White, 1985), maize tonoplast H^+-ATPase (59; Tu et al., 1988) and bovine tubulin GTPase (88; Mejillano, Shivanna & Himes, 1996).

The effects of nucleotide mixtures on locking open and the asymmetric temperature dependencies of channel opening and closing rates reported here suggest regulation by two functionally distinct sites. The asymmetrical temperature dependencies of channel opening and closing are consistent with two distinct temperature-dependent reaction steps, and therefore compatible with a cyclic gating scheme. This result is significant since several linear models have been proposed (Fischer & Machen, 1994; Venglarik et al., 1994; Schultz et al., 1995) and, although most appealing, there is only indirect evidence for a cyclic scheme. Extending the present experiments to mutant CFTR channels with altered NBFs should yield further information concerning the role of each domain in the gating cycle and locking.

We thank Drs. Xiu-Bao Chang and John Riordan (Mayo Clinic Scottsdale, Scottsdale, AZ) for providing the CHO cell lines expressing WT and 10SA CFTR and Jie Liao for cell culture.

References

Acerbo, P., Nobile, M. 1994. Temperature dependence of multiple high voltage activated Ca^{2+} channels in chick sensory neurones. *Eur. Biophys. J.* **23:**189–195

Anderson, M.P., Berger, H.A., Rich, D.P., Gregory, R.J., Smith, A.E., Welsh, M.J. 1991. Nucleoside triphosphates are required to open the CFTR chloride channel. *Cell* **67:**775–784

Baukrowitz, T., Hwang, T.-C., Nairn, A.C., Gadsby, D.C. 1994. Coupling of CFTR Cl^- channel gating to an ATP hydrolysis cycle. *Neuron* **12:**473–482

Berger, H.A., Travis, S.M., Welsh, M.J. 1993. Regulation of the cystic fibrosis transmembrane conductance regulator Cl^- channel by specific protein kinases and phosphatases. *J. Biol. Chem.* **268:**2037–2047

Bukauskas, F.F., Elfgang, C., Willecke, K., Weingart, R. 1995. Biophysical properties of gap junction channels formed by mouse connexin40 in induced pairs of transfected human HeLa cells. *Biophys. J.* **68:**2289–2298

Carson, M.R., Travis, S.M., Welsh, M.J. 1995. The two nucleotide-binding domains of CFTR have distinct functions in controlling channel activity. *J. Biol. Chem.* **270:**1711–1717

Carson, M.R., Welsh, M.J. 1995. Structural and functional similarities between the nucleotide-binding domains of CFTR and GTP-binding proteins. *Biophys. J.* **69:**2443–2448

Chang, X.-B., Tabcharani, J.A., Hou, Y.-X., Jensen, T.J., Kartner, N., Alon, N., Hanrahan, J.W., Riordan, J.R. 1993. Protein kinase A (PKA) still activates CFTR chloride channel after mutagenesis of all ten PKA consensus phosphorylation sites. *J. Biol. Chem.* **268:**11304–11311

Cheng, S.H., Rich, D.P., Marshall, J., Gregory, R.J., Welsh, M.J., Smith, A.E. 1991. Phosphorylation of the R domain by cAMP-dependent protein kinase regulates the CFTR chloride channel. *Cell* **66:**1027–1036

Dousmanis, A.G., Nairn, A.C., Gadsby, D.C. 1996. $[Mg^{2+}]$ governs CFTR Cl^- channel opening and closing rates, confirming hydrolysis of two ATP molecules per gating cycle. *Biophys. J.* **70:**A127(*Abstr.*)

Fischer, H., Machen, T.E. 1994. CFTR displays voltage dependence and two gating modes during stimulation. *J. Gen. Physiol.* **104:**541–566

Friedrich, T., Bamberg, E., Nagel, G. 1996. Na^+, K^+-ATPase pump currents in giant excised patches activated by an ATP concentration jump. *Biophys. J.* **71:**2486–2500

Gadsby, D.C., Nagel, G., Hwang, T.-C. 1995. The CFTR chloride channel of mammalian heart. *Annu. Rev. Physiol.* **57:**387–416

Gray, M.A., Greenwell, J.R., Argent, B.E. 1988. Secretin-regulated chloride channel on the apical plasma membrane of pancreatic duct cells. *J. Membrane Biol.* **105:**131–142

Gunderson, K.L., Kopito, R.R. 1994. Effects of pyrophosphate and nucleotide analogues suggests a role for ATP hydrolysis in cystic fibrosis transmembrane regulator channel gating. *J. Biol. Chem.* **269:**19349–19353

Hamill, O.P., Marty, A., Neher, E., Sakmann, B., Sigworth, F.J. 1981. Improved patch-clamp techniques for high-resolution current recording from cells and cell-free membrane patches. *Pfluegers Arch.* **391:**85–100

Hanrahan, J.W., Tabcharani, J.A., Becq, F., Mathews, C.J., Augustinas, O., Jensen T.J., Chang, X.-B., Riordan, J.R. 1995. Function and dysfunction of the CFTR chloride channel. In: Ion Channels and Genetic Diseases. D.C. Dawson and R.A. Frizzell, editors. pp. 125–137. New York: Rockefeller Univ. Press

Hanrahan, J.W., Kon, Z., Mathews, C.J., Luo, J., Jia, Y., Linsdell, P. 1998. Patch clamp studies of the CFTR chloride channel. *Meths. Enz.* (*in press*)

Haverkampf, K., Benz, I., Kohlhardt, M. 1995. Thermodynamically specific gating kinetics of cardiac mammalian $K^+_{(ATP)}$ channels in a physiological environment near 37°C. *J. Membrane Biol.* **146:**85–90.

Hille, B. 1992. Ionic Channels of Excitable Membranes. *Sinauer Associates, Sunderland, MA*

Hwang, T.-C., Nagel, G., Nairn, A.C., Gadsby, D.C. 1994. Regulation of the gating of cystic fibrosis transmembrane conductance regulator Cl channels by phosphorylation and ATP hydrolysis. *Proc. Natl. Acad. Sci. USA* **91:**4698–4702

Hyde, S.C., Emsley, P., Hartshorn, M.J., Mimmack, M.M., Gileadi, U., Pearce, S.R., Gallagher, M.P., Gill, D.R., Hubbard, R.E., Higgins, C.F. 1990. Structural model of ATP-binding proteins associated with cystic fibrosis, multidrug resistance and bacterial transport. *Nature* **346:**362–365

Jia, Y., Mathews, C.J., Hanrahan, J.W. 1997. Phosphorylation by protein kinase C is required for acute activation of cystic fibrosis transmembrane conductance regulator by protein kinase A. *J. Biol. Chem.* **272:**4978–4984

Li, C., Ramjeesingh, M., Wang, W., Garami, E., Hewryk, M., Lee, D., Rommens, J.M., Galley, K., Bear, C.E. 1996. ATPase activity of the cystic fibrosis transmembrane conductance regulator. *J. Biol. Chem.* **271:**28463–28468

Manavalan, P., Dearborn, D.G., McPherson, J.M., Smith, A.E. 1995. Sequence homologies between nucleotide binding regions of CFTR and G-proteins suggest structural and functional similarities. *FEBS Lett.* **366:**87–91

Mathews, C.J., Tabcharani, J.A., Chang, X.-B., Riordan, J.R., Hanrahan, J.W. 1995. Models for gating of CFTR chloride channels. *Ped. Pulmonol.* **20:**424(*Abstr.*)

Mathews, C.J., Tabcharani, J.A., Chang, X.-B., Riordan, J.R., Hanrahan, J.W. 1996. Characterization of nucleotide interactions with CFTR channels. *Ped. Pulmonol.* **Suppl. 13:**221(*Abstr.*)

Mathews, C.J., Tabcharani, J.A., Chang, X.-B., Riordan, J.R., Hanrahan, J.W. 1998. Phosphorylation-dependent gating of CFTR by nucleotides. *J. Physiol.* (*in press*)

Mejillano, M.R., Shivanna, B.D., Himes, R.H. 1996. Studies on the nocodazole-induced GTPase activity of tubulin. *Arch. Biochem. Biophys.* **336:**130–138

Nagel, G., Hwang, T.-C., Nairn, A.C., Gadsby, D.C. 1994. AMP-PNP delays the closing of CFTR Cl channels opened by ATP. *Biophys. J.* **66:**A141(*Abstr.*)

Nagy, K., Kiss, T., Hof, D. 1983. Single Na channels in mouse neuroblastoma cell membrane. *Pfluegers Arch.* **399:**302–308

Otis, T.S., DeKoninck, Y., Mody, I. 1993. Characterization of synaptically elicited $GABA_B$ responses using patch-clamp recordings in rat hippocampal slices. *J. Physiol.* **463:**391–407

Picciotto, M.R., Cohn, J.A., Bertuzzi, G., Greengard, P., Nairn, A.C. 1992. Phosphorylation of the cystic fibrosis transmembrane conductance regulator. *J. Biol. Chem.* **267:**12742–12752

Pusch, M., Ludewig, U., Jentsch, T.J. 1997. Temperature dependence of fast and slow gating relaxations of ClC-0 chloride channels. *J. Gen. Physiol.* **109:**105–116

Reddy, M.M., Quinton, P.M. 1994. Rapid regulation of electrolyte absorption in sweat duct. *J. Membrane Biol.* **140:**57–67

Riordan, J.R., Rommens, J.M., Kerem, B.-S., Alon, N., Rozmahel, R., Grzelczak, Z., Zielenski, J., Lok, S., Plavsic, N., Chou, J.-L.,

Drumm, M.L., Iannuzzi, M.C., Collins, F.S., Tsui, L.-C. 1989. Identification of the cystic fibrosis gene: Cloning and characterization of complementary DNA. *Science* **245:**1066–1073

Schultz, B.D., Venglarik, C.J., Bridges, R.J., Frizzell, R.A. 1995. Regulation of CFTR Cl^- channel gating by ADP and ATP analogues. *J. Gen. Physiol.* **105:**329–361

Schwarz, J.R., Eikhof, G. 1987. Na currents and action potentials in rat myelinated nerve fibres at 20 and 37°C. *Pfluegers Arch.* **409:**569–577

Siemankowski, R.F., Wiseman, M.O., White, H.D. 1985. ADP dissociation from actomyosin subfragment 1 is sufficiently slow to limit the unloaded shortening velocity in vertebrate muscle. *Proc. Natl. Acad. Sci. USA* **82:**658–662

Tabcharani, J.A., Chang, X.-B., Riordan, J.R., Hanrahan, J.W. 1991. Phosphorylation-regulated Cl^- channel in CHO cells stably expressing the cystic fibrosis gene. *Nature* **352:**628–631

Tabcharani, J.A., Low, W., Elie, D., Hanrahan, J.W. 1990. Low-conductance chloride channel activated by cAMP in the epithelial cell line T_{84}. *FEBS Lett.* **270:**157–164

Tu, S.-I., Brouillette, J.N., Nagahashi, G., Brauer, D., Nungesser, E. 1988. Temperature dependence and mercury inhibition of tonoplast-type H^+-ATPase. *Arch. Biochem. Biophys.* **266:**289–297

Venglarik, C.J., Schultz, B.D., Frizzell, R.A., Bridges, R.J. 1994. ATP alters current fluctuations of cystic fibrosis transmembrane conductance regulator: Evidence for a three-state activation mechanism. *J. Gen. Physiol.* **104:**123–146

Weber, J., Senior, A.E. 1996. F_1F_0-ATP synthase: development of direct optical probes of the catalytic mechanism. *Biochim. Biophys. Acta* **1275:**101–104

Welsh, M.J., Smith, A.E. 1994. Molecular mechanisms of CFTR chloride channel dysfunction in cystic fibrosis. *Cell* **73:**1251–1254